Negative Catalytic Effect of Water on the Reactivity of Hydrogen Abstraction from the C–H Bond of Dimethyl Ether by Deuterium Atoms through Tunneling at Low Temperatures

Yasuhiro Oba, Naoki Watanabe, Akira Kouchi*

Institute of Low Temperature Science, Hokkaido University, N19W8, Kita-ku, Sapporo, Hokkaido 060-0819 Japan

Corresponding Author

*Yasuhiro Oba (oba@lowtem.hokudai.ac.jp).

ABSTRACT. We report an experimental study on the catalytic effect of solid water on the reactivity of hydrogen abstraction (H-abstraction) from dimethyl ether (DME) in the low-temperature solid DME–H_2O complex. When DME reacted with deuterium atoms on a surface at 15–25 K, it was efficiently deuterated via successive tunneling H-abstraction and deuterium (D)-addition reactions. The “effective” rate constant for DME–H_2O + D was found to be about 20 times smaller than that of pure DME + D. This provides the first evidence that the presence of solid water has a negative catalytic effect on tunneling H-abstraction reactions.

1. INTRODUCTION

Water is ubiquitously distributed not only on Earth but also in extraterrestrial environments such as planetary systems and interstellar space. In the coldest region of interstellar space, where the typical temperature is as low as 10 K, water is present in the amorphous solid state as an ice mantle of interstellar grains [1]. Amorphous solid water (ASW) is known to play a crucial role in promoting the formation of various molecules on cold interstellar grains. For instance, previous studies have experimentally demonstrated that the successive additions of hydrogen (H) atoms to solid carbon monoxide (CO), producing formaldehyde (H_2CO) and methanol (CH_3OH), are enhanced on the ASW surface relative to the pure CO solid [2]. In this reaction system, both H atoms and CO molecules are physisorbed on the ASW surface due to van der Waals interactions. In addition to such a physisorption system, water can form a complex with other molecules via hydrogen bonds (H-bonds) owing to its large dipole moment. Since H-bonding (typical binding energy: <20–25 kJ mol^{-1} [3]) is generally stronger than van der Waals interactions, it may have a different catalytic effect for the chemical reactions of molecules forming a H-bond with water. For example, theoretical studies have reported that water clusters lower the activation barriers of chemical reactions such as hydrogen addition to a H_2CO–water complex [4]. Furthermore, the rate of the reaction between hydroxyl radicals and acetaldehyde in the gas phase is significantly enhanced in the presence of a water molecule due to the formation of a H-bond [5]. H-bonds also play a catalytic role in the low-temperature formation of various complex organic molecules (COMs) such as glycine [6]. Moreover, there are other cases where the presence of a H-bond reduces the activation barrier of some reactions at low temperatures even in the absence of water [e.g., 7]. Nevertheless, due to the current lack of studies on these reactions, the effect of

the H-bond with water on chemical reactions at low temperatures remains to be understood. Thus, it is desirable to elucidate the influence of ASW-molecule complex formation via H-bonding in order to obtain a better understanding of chemical evolution on interstellar icy grains.

In the present study, we report experimental results for the surface reactions of a dimethyl ether (DME: CH_3OCH_3)–water complex or pure solid DME with deuterium (D) atoms at 15–25 K to reveal a possible catalytic effect of the H-bond with water on the reaction. DME, which is one of the most abundant COMs in interstellar space, is known to form a H-bond with water linking the DME oxygen atom and the hydrogen atom of water [8]. In the reaction of DME with D atoms, we expect successive H-abstraction and D-addition reactions (H-D substitution) to occur on the low-temperature surface (Figure 1). This type of reaction on interstellar grains plays a crucial role in the chemical evolution toward deuterium enrichment of interstellar molecules. Despite a large activation barrier (>20 kJ mol^{-1}) for the first H-abstraction reaction, these reactions are known to occur via the quantum tunneling effect for several organic molecules such as methanol [10,11], formaldehyde [12], methylamine [13], glycine [14], and ethanol [15]. In addition, several experimental and theoretical studies have demonstrated that quantum tunneling plays an important role in various chemical systems, especially at low temperatures [e.g., 16–20]. Since an interstellar DME molecule is found to be highly deuterium-enriched (CH_3OCH_2D/CH_3OCH_3 = ~15% [21]), H-D substitution should be examined for the deuterium enrichment of DME.

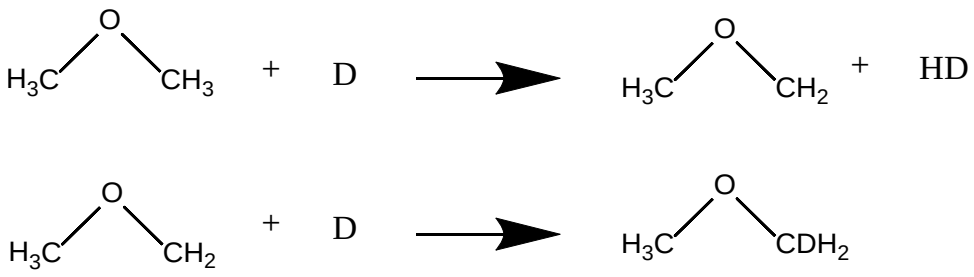

Figure 1. H-abstraction reaction from the methyl group of dimethyl ether by D atoms, followed by the addition of a D atom to the formed CH_3OCH_2 radical. The abstraction reaction has a large activation barrier of ~3600 K (~30 kJ mol^{-1} [9]) in the gas phase.

2. EXPERIMENTAL METHODS

All reactions were performed in an experimental apparatus named Apparatus for Surface Reactions in Astrophysics (ASURA), whose description is detailed elsewhere [11]. In brief, ASURA consists of a reaction chamber, an atomic-source chamber, multiple turbo molecular pumps, a quadrupole mass spectrometer (QMS), and a Fourier-transform infrared (FTIR) spectrometer. The base pressure of the reaction chamber is of the order of 10^{-8} Pa. An aluminum substrate, whose temperature can be controlled from 5 to 300 K, is mounted at the center of the reaction chamber. For the reaction of pure DME with D atoms, gaseous DME (99.9%, Takachiho Chemical Industrial Co., Ltd.) was vapor-deposited onto the substrate at 15 K through a capillary plate. The column density of DME was estimated to be ~1×10^{16} molecules cm^{-2}. In the experiments for the DME–H_2O complex, DME gas was premixed with distilled and deionized H_2O in a sample preparation chamber with an approximate ratio of 1 (DME):4 (water), and was vapor-deposited onto the substrate at 15 K. Based on the peak area and band strength for the 3 μm band of H_2O [22], the H_2O column density was estimated as ~2×10^{16} molecules cm^{-2}.

The samples were exposed to D atoms produced in an atomic source by dissociation of D_2 molecules in microwave-induced plasma and cooled to 100 K through a cold pipe. The flux of D atoms was estimated as $1.7 \pm 0.4 \times 10^{15}$ atoms cm^{-2} s^{-1} using the procedure described in ref. [23]. The samples were exposed to D atoms for up to 240 min, and gaseous samples desorbed from the substrate were monitored by QMS.

3. RESULTS AND DISCUSSION

Figure 2 shows the FTIR spectra of a pure DME solid and a DME/H_2O mixture deposited at 15 K, with the CH_3-stretching frequency region (~2800 cm^{-1}) enlarged in the inset of the figure. Although the CH_3-stretching band for the DME/H_2O mixture is superimposed on the tail of the strong 3-μm band of H_2O, the CH_3-stretching frequency (2828 cm^{-1}) is clearly blue-shifted by 12 cm^{-1} from that of the pure DME solid (2816 cm^{-1}), which indicates the formation of a DME–H_2O complex in the solid sample [8]. The observed peak shift is consistent with previous experimental [8,24] and theoretical [25] studies.

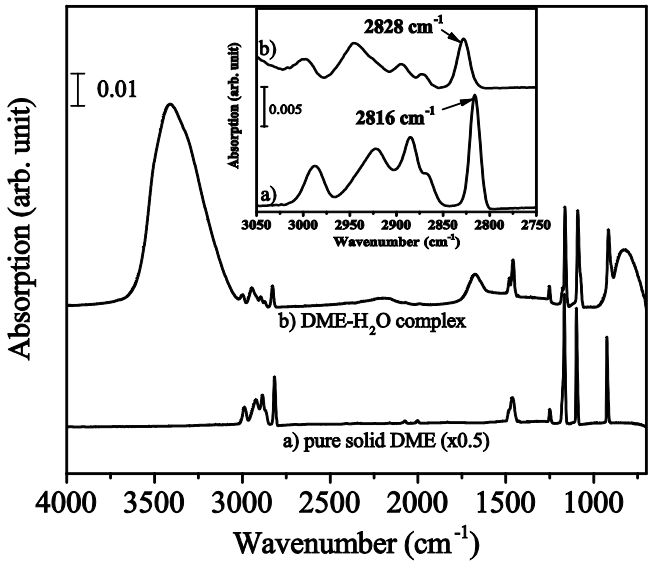

Figure 2. FTIR spectra of (a) pure solid DME and (b) DME–H_2O complex produced by vapor deposition at 15 K. Inset shows the CH_3-stretching region of the same samples at 2750–3050 cm^{-1}. The spectrum of pure solid DME is scaled by 0.5 to allow better comparison with the complex.

Figure 3 shows variations in the difference spectra (2000–3100 cm^{-1}) of pure solid DME exposed to D atoms at 15 K. With increasing D exposure times, the intensity of the CH_3-stretching band decreases. At the same time, new C-D-stretching bands appear at around 2000–2200 cm^{-1}. These results indicate that H-D substitution reactions (Figure 1) occurred at

15 K. Temperature-programmed desorption experiments confirm the formation of deuterated DME as CD_3OCD_3, a fully deuterated dimethyl ether (Figure 4).

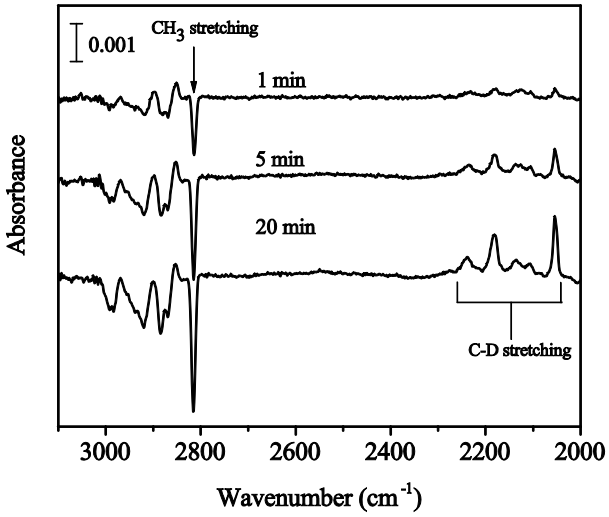

Figure 3. Variations in the difference spectra of pure solid DME after exposure to D atoms for up to 20 min at 15 K.

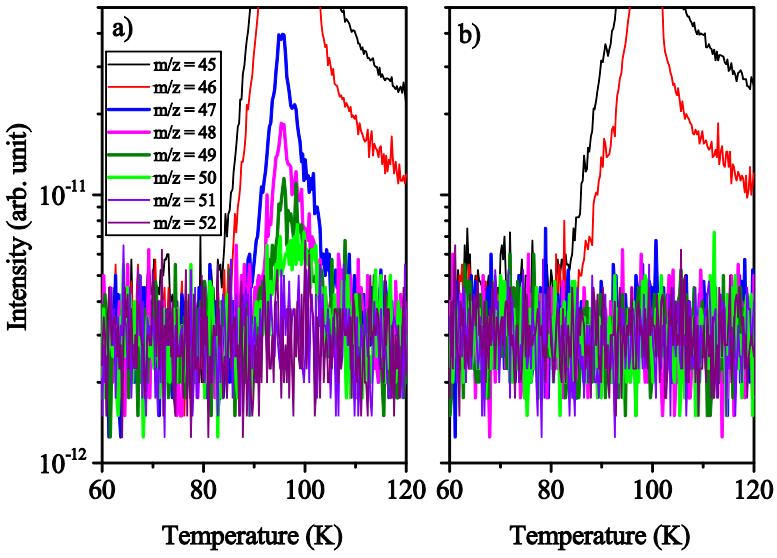

Figure 4. Temperature-programmed desorption spectra of pure DME solid (a) with and (b) without exposure to D atoms at 15 K. The peak increase of m/z = 47 to 50 for the D-exposed sample suggests the formation of deuterated DME. The peak for m/z = 50 mainly

corresponds to $CD_3OCD_2^+$, whose parent molecule is the fully deuterated DME CD_3OCD_3 (m/z = 52).

Figure 5 shows variations in the column density of pure solid DME after exposure to D atoms at 15–25 K. Based on the number of reacted molecules and the total dose of D atoms, we conclude that D atoms are in excess of solid DME under the present experimental conditions. This is based on the fact that only approximately 10^{-5} of the total D atoms were consumed by the reaction. That is, the surface number density of D atoms ([D]) is constant for the entire duration of the experiment and is dominated by the balance between the incoming flux and loss by D-D recombination (D_2 formation) and D atom desorption, as described by eq. (1) [26] (See Supporting Information for further details):

$$p_s F_D = k_{D+D}[D]^2 + k_{des}[D], \qquad (1)$$

where p_s, F_D, k_{D+D}, and k_{des} represent the D-atom sticking coefficient, the flux of D atoms, the rate constant of D + D recombination, and the rate constant of monoatomic desorption from the surface, respectively. Therefore, this can be reasonably assumed to be a pseudo-first-order reaction, and thus, the plots should be fitted by a single exponential decay function:

$$N_t/N_0 = A(1\text{-}e^{-kt}), \qquad (2)$$

where N_t, N_0, A, and k represent the column density of DME at times t and t = 0, the saturation value, and the effective rate constant, respectively. The term k can be expanded into k' × [D], where k' represents the actual rate constant [2]. Since [D] cannot be determined in the present experiment, the value of k (in min^{-1}) is used as a fitting parameter.

The plots in Figure 5 could not be successfully fitted by a single exponential function (2), implying the presence of both reactive (fast decay) and less-reactive (slow decay) DME molecules on the upper-most surface and those embedded in lower layers, respectively. As a result, the effective rate constant k_{pure} in pure solid DME experiment was derived from the

fitting of the plots in Figure 5 by a double-component exponential decay function for the decreases in both reactive and less-reactive parent molecules (for details, see Supporting Information).

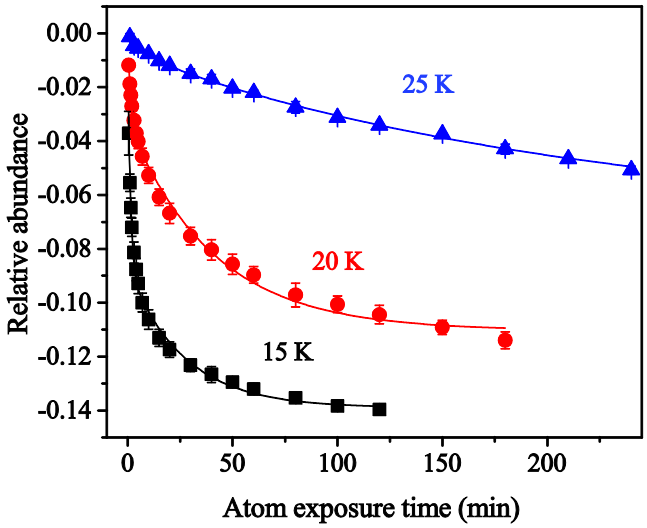

Figure 5. Variations in the column density of pure solid DME normalized to the initial abundance with atom exposure times at 15–25 K. Solid lines represent the least-square fitting of the plots by the double-component single exponential decay function. Error bars represent statistical errors.

The value of fast decay k_{pure} (min^{-1}) was 8.3×10^{-1} at 15 K and dropped to 6.9×10^{-1} and 1.1×10^{-1} at 20 and 25 K, respectively. The decline in k_{pure} is likely due to the decrease in [D] with increasing substrate temperature. A temperature dependence of the rate of surface reactions has often been observed in similar experiments at low temperatures [2].

H-D substitution also occurred for DME in the DME–H_2O complex (Figure S2). Figure 6 plots the variation in the normalized column density of the DME–H_2O complex after exposure to D atoms at 15 K, together with that of pure solid DME at 15 K for comparison. Variations in DME abundance in the complex are shown for various temperatures in Figure S3. In contrast to the case of pure solid DME + D, plots for the DME–H_2O complex can be

fitted by a single exponential decay function (2) to obtain the value of k (hereafter denoted as $k_{comp} = k'_{comp} \times [D]$, where k'_{comp} represents the actual rate constant for the reaction of the DME–H_2O complex with D atoms). The difference in decay (single or double components) behaviors may originate from the difference in the structures of the sample solids; in the present study, pure DME solid is amorphous and likely has a porous structure, yielding different reactivities depending on the location in the solid. In contrast, although H_2O and DME are amorphous in the complex, as indicated by the shape of the IR bands [8,24,27], the complex is considered to be more compact than pure solid DME. This is inferred from the weak intensity of the dangling OH band for the complex (Figure 7). In this case, D atoms do not often diffuse into the bulk solid, and hence, H-D substitution occurred mostly on the outermost surface of the complex. As a result, k_{comp} should be compared with k_{pure} for fast decay. The value obtained for k_{comp} was 4.0×10^{-2} at 15 K, about 20 times smaller than the value of k_{pure} at the same temperature. This provides clear evidence for a negative catalytic effect of water on the effective rate constant for DME + D under the present experimental conditions. The k_{comp} value dropped with increasing sample temperature, as is also observed in the pure DME experiment (Figure 8). This decrease is also explained by the decrease in [D] with temperature. The observed variations in k with temperature indicate that the H-D substitution reaction proceeds via the Langmuir–Hinshelwood mechanism, not via the Eley–Rideal mechanism, because the latter generally shows little surface temperature dependence.

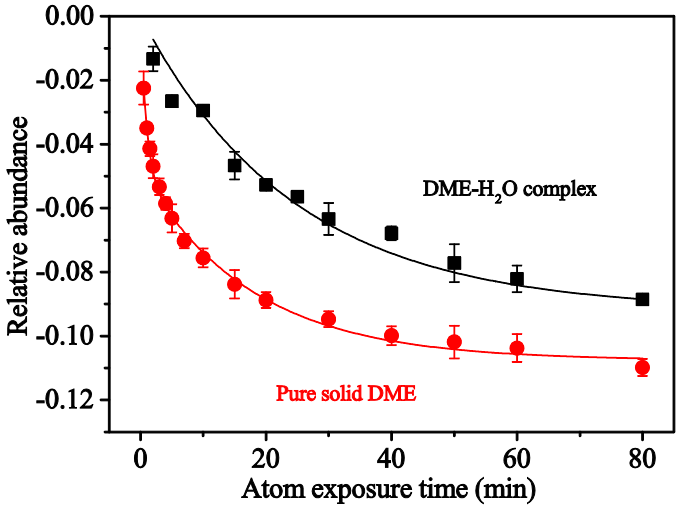

Figure 6. Variations in the column density of pure DME (filled circle) and DME in the complex with H_2O (filled square) normalized to the initial column density, with atom exposure times at 15 K. Solid lines represent the least-square fitting of DME attenuation to the single exponential function. Error bars represent statistical errors.

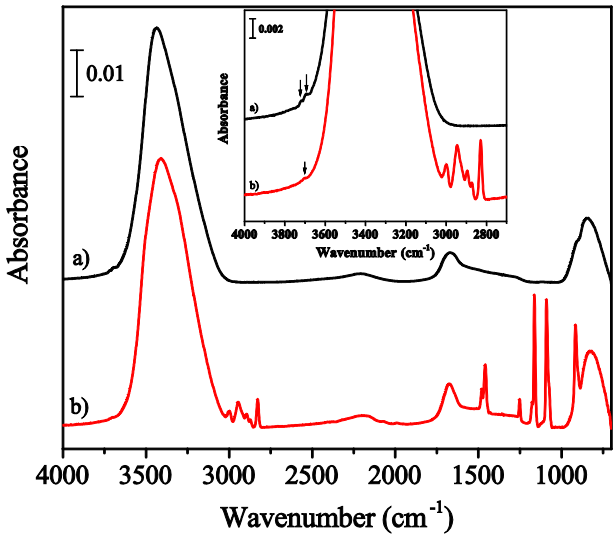

Figure 7. FTIR spectra of (a) vapor-deposited ASW and (b) the DME–H_2O complex. Both solid samples were deposited at 15 K. The inset shows enlarged spectra of the same samples

at 2700–4000 cm^{-1}. Arrows in the inset indicate the dangling OH bands, with two peaks (3695 and 3719 cm^{-1}) for ASW and one peak (3703 cm^{-1}) for the DME–H_2O complex.

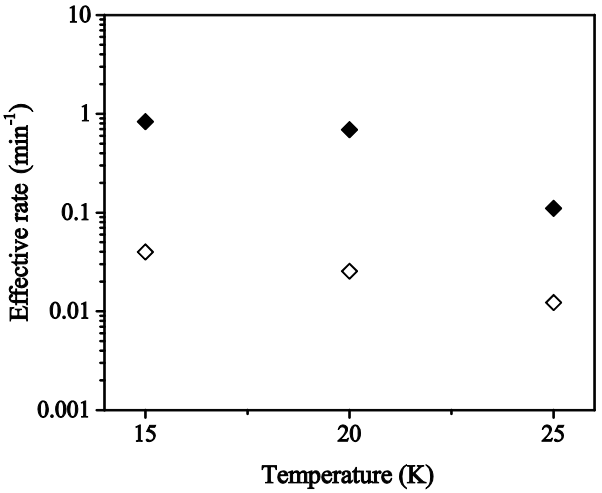

Figure 8. Variations in the effective rate constant k (in min^{-1}) for the reaction of pure solid DME (k_{pure}: filled diamond) and DME–H_2O complex (k_{comp}: open diamond), with D atoms at 15–25 K.

The fitting parameter k_x (x = pure or comp) is the product of k'_x and [D]; hence, if [D] is equivalent in the two reaction systems, k'_{pure} is about 20 times larger than k'_{comp}. Although the D atom fluxes were the same for each experiment, it is not obvious that the surface number density [D] was also precisely equivalent. Unfortunately, the absolute value of [D] cannot be measured in the present study, as mentioned earlier; however, because D atoms mostly physisorb on both pure solid DME and the DME–H_2O complex, the adsorption energy of D atoms on pure solid DME should not differ significantly from that on the DME–H_2O complex. Thus, [D] on pure solid DME would be comparable to that on the DME–H_2O solid. As a result, instead measuring D atoms, we compared the absorption energy of H_2 on pure solid DME to that on the DME–H_2O complex because the H_2 molecule has the same mass as

that of a D atom and adsorbs on these solids via van der Waals interaction. After equal amounts of H_2 were deposited on each solid at 10 K, H_2 was detected by a thermal desorption method. The thermal desorption profiles of H_2 from both solids provide information about the absorption energy of H_2.

Figure 9 shows thermal desorption profiles of H_2 from pure DME and the DME–H_2O complex with the same thickness as in the respective H-D substitution experiments shown above. Although H_2 began to desorb from each solid soon after the temperature increased, the peak temperature was slightly higher for the DME–H_2O complex relative to pure DME. This result implies that the absorption energy of H_2 on the DME–H_2O complex is very similar to, or slightly higher than, that on pure DME solid. This leads to a reasonable assumption that the number density of D atoms on the DME–H_2O complex is identical to, or higher than, that on pure DME solid. Nevertheless, k_{comp} is actually much smaller than k_{pure} (Figure 8), implying that k'_{comp} is more than 20 times smaller than k'_{pure} due to the formation of a complex with H_2O via H-bonds. Further studies are highly necessary to more quantitatively evaluate the catalytic effect of water on the rate constant of the DME + D reaction.

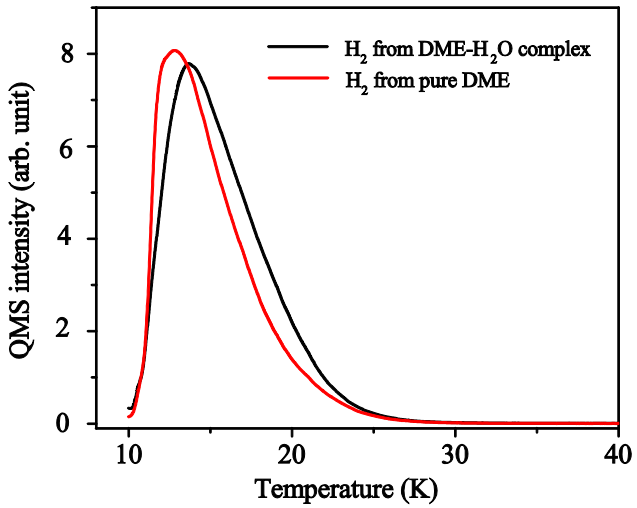

Figure 9. Thermal desorption spectra of H_2 from pure solid DME (red) and DME–H_2O complex (black).

Due to a large activation barrier of ~3600 K (~30 kJ mol^{-1}) for the H-abstraction reaction (Figure 1) [9], this reaction should proceed through quantum tunneling at temperatures as low as 15 K. For simplicity, assuming a rectangular potential barrier with width a and height E_a for the reaction, the rate of quantum tunneling k_q can be roughly estimated from the following function [2,28]:

$$k_q \approx \nu_0 \exp[-(2a/\hbar)(2mE_a)^{1/2}], \quad (3)$$

where ν_0 and m represent the harmonic frequency and tunneling mass, respectively. As can be seen in eq. (3), the tunneling rate strongly depends on the tunneling mass and barrier shape. Since the chemical reaction itself is the same in the two experiments (i.e., H-abstraction from DME by a D atom), the tunneling mass is the same. Likewise, ν_0 is expected to be similar in each case. In contrast, the potential width and height for the H-abstraction reaction may vary depending on the presence or absence of a H-bond with H_2O. When DME forms a complex with H_2O via a H-bond, where the oxygen atom of DME and a hydrogen atom of water act as the proton acceptor and donor, respectively, the lone-pair electron density of DME oxygen decreases, resulting in the relaxation of the intramolecular hyperconjugation between the lone-pair electrons of the DME oxygen and the σ-bond of the methyl group [8,29]. This is accompanied by a lengthening of the C–O bond in DME and the propagation of the relaxation to the methyl group, resulting in the contraction of the C–H bond [8,25,30]. Since the contraction of a bond generally leads to its strengthening, the C–H bond becomes stronger in the complex, which would have a dominant contribution to the observed difference between k_{pure} and k_{comp}.

A simple DFT calculation suggests that the activation barrier for H- abstraction from the DME–water complex by a D atom is about twice as large as that from pure DME [31]. In

addition, Woon [4] performed quantum chemical calculations in a similar reaction system to study the effect of water on H-abstraction from H_2CO by H atoms. The activation barrier for the H-abstraction reaction

$$H_2CO + H \rightarrow H_2 + HCO \qquad (4)$$

increases by ~4 kJ mol^{-1} in the presence of water molecules [4]. This may be explained by the same reason for the case of DME because the C–H bond in H_2CO is considered to contract as a result of H-bond formation with water [32]. These calculations are consistent with the present results, which state that the reactivity for DME–water complex + D is much lower than that for pure DME + D.

Note that the 12 cm^{-1} blue shift of the C–H bond stretch observed in the present study corresponds to the contraction of the C–H bond by ~1×10^{-3} Å [25]. This suggests that this slight change can change tunneling probablity for the reaction. Since the degree of bond contraction induced by the formation of a H-bond depends significantly on the molecule [29], the efficiencies of reactions involving H-abstraction from the C–H bond of hydrogen-bonded molecules may also vary. In the quantitative studies of chemical reactions in interstellar molecular clouds, where molecules may form a complex with ASW via a H-bond, the effect of complex formation must be carefully considered in order to avoid a drastic underestimation of the reaction efficiency. Further theoretical and experimental studies are therefore necessary for more quantitative understanding of chemical reactions of molecules with blue-shifted C–H bonds.

4. CONCLUSION

We experimentally studied the reactions of pure solid DME and a solid DME–H_2O complex with deuterium atoms at low temperatures (15–25 K) to elucidate the possible catalytic effects of solid water on the reactivity of DME with D atoms on a low-temperature

surface. Carbon-bound hydrogen of DME was abstracted by D atoms via quantum tunneling, followed by the addition of another D atom to yield deuterated DME. The effective rate constant for the DME–H_2O complex with D atoms was about 20 times smaller than that for pure DME solid at 15 K. The reduction in reactivity is attributed to the negative catalytic effect of solid water via the formation of a H-bond between the hydrogen atom of water and the oxygen atom of DME, resulting in the strengthening of the C–H bond in the DME–H_2O complex.

ASSOCIATED CONTENT

Supporting Information. Information about the fitting function, number density of D atoms on the solid surfaces, additional figures and references.

ACKNOWLEDGMENT

The authors thank Dr. Y. Osamura for performing quantum chemical calculations for the H-abstraction from pure DME and DME–water complex. This study was supported by a Grant-in-Aid for Scientific Research from the Ministry of Education, Culture, Sports, Science and Technology of Japan and the Japan Society for the Promotion of Science (JSPS KAKENHI Grant Number JP26108501).

REFERENCES

[1] Gibb, E. L.; Whittet, D. C. B.; Boogert, A. C. A.; Tielens, A. G. G. M. *Astrophys. J. Suppl. Ser.* **2004**, 151, 35–73.

[2] Watanabe, N.; Kouchi, A. *Prog. Surf. Sci.* **2008**, 83, 439–489.

[3] Muller, P. *Pure & Appl. Chem.*, **1994**, 66, 1077–1184.

[4] Woon, D. E. *Astrophys. J.* **2002**, 569, 541–548.

[5] Vöhringer-Martinez, E.; Hansmann, B.; Hernandez, H.; Francisco, J. S.; Abel, B. *Scienc*e **2007**, 315, 497–501.

[6] Rimola, A.; Sodupe, M.; Ugliengo, P. *Astrophys. J.* **2012**, 754, 24.

[7] Shannon, R. J.; Goddard, M. A.; Heard, D. E. *Nat. Chem.* **2013**, 5, 745–749.

[8] Barnes, A. J.; Beech, T. R. *Chem. Phys. Lett.* **1983**, 94, 568–570.

[9] Saheb, V. *J. Phys. Chem. A* **2015**, 119, 4711–4717.

[10] Nagaoka, A.; Watanabe, N.; Kouchi, A. *Astrophys. J. Lett.* **2005**, 624, L29–L32.

[11] Nagaoka, A.; Watanabe, N.; Kouchi, A. *J. Phys. Chem. A* **2007**, 111, 3016–3028.

[12] Hidaka, H.; Watanabe, M.; Kouchi, A.; Watanabe, N. *Astrophys. J.* **2009**, 702, 291–300.

[13] Oba, Y.; Chigai, T.; Osamura, Y.; Watanabe, N.; Kouchi, A. *Meteor. Planet. Sci.* **2014**, 49, 117–132.

[14] Oba, Y.; Watanabe, N.; Osamura, Y.; Kouchi, A. *Chem. Phys. Lett.* **2015**, 634, 53–59.

[15] Oba, Y.; Osaka, K.; Chigai, T.; Kouchi, A.; Watanabe, N. *Mon. Not. Roy. Astron. Soc.* **2016**, in press. DOI: 10.1093/mnras/stw1714.

[16] Schreiner, P. R.; Reisenauer, H. P.; Ley, D.; Gerbig, D.; Wu, C.-H.; Allen, W. D. *Science* **2011**, 332, 1300–1303.

[17] Mutunga, F. M.; Follett, S. E.; Anderson, D. T. *J. Chem. Phys.* **2013**, 139, 151104.

[18] Meisner, J.; Kästner, J. *Angew. Chem. Int. Ed.* **2016**, 55, 5400–5413.

[19] Momose, T.; Hoshina, H.; Sogoshi, N.; Katsuki, H.; Wakabayashi, T.; Shida, T. *J. Chem. Phys.* **1998**, 108, 7334–7338.

[20] Hidaka, H.; Kouchi, A.; Watanabe, N. *J. Chem. Phys.* **2007**, 126, 204707.

[21] Richard, C.; Margulès, L.; Cauz, E.; Kahane, C.; Ceccarelli, C.; Guilemin, J.-C.; Motiyenko, R. A.; Vastel, C.; Groner, P. *Astron. Astrophys.* **2013**, 552, A117.

[22] Gerakines, P. A.; Schutte, W. A.; Greenberg, J. M.; van Dishoeck, E. F. *Astron. Astrophys.* **1995**, 296, 810–818.

[23] Oba, Y.; Osaka, K.; Watanabe, N.; Chigai, T.; Kouchi, A. *Faraday Discuss.* **2014**, 168, 185–204.

[24] Schriver-Mazzuoli, L.; Coanga, J. M.; Schriver, A.; Ehrenfreund, P. *Vib. Spectrosc.* **2002**, 30, 245–257.

[25] Karpfen, A.; Kryachko, E. S. *Chem. Phys. Lett.* **2006**, 431, 428–433.

[26] Kuwahata, K.; Hama, T.; Kouchi, A.; Watanabe, N. *Phys. Rev. Lett.* **2015**, 115, 133201.

[27] Hagen, W.; Tielens, A. G. G. M.; Greenberg, J. M. *Chem. Phys.* **1981**, 56, 367–379.

[28] Hama, T.; Watanabe, N. *Chem. Rev.* **2013**, 113, 8783–8839.

[29] Hobza, P.; Havlas, Z. *Chem. Rev.* **2000**, 100, 4253–4264.

[30] Barnes, A. J. *J. Mol. Struct.* **2004**, 704, 3–9.

[31] Osamura, Y. **2016**, private communication.

[32] Scheiner, S.; Kar, T. *J. Phys. Chem. A* **2008**, 112, 11854–11860.